Author/s:
Goodall, KJ;Nguyen, A;Matsumoto, A;McMullen, JR;Eckle, SB;Bertolino, P;Sullivan, LC;Andrews, DM

Title:
Multiple receptors converge on H2-Q10 to regulate NK and γδT-cell development

Date:
2019-03-01

Citation:
Goodall, K. J., Nguyen, A., Matsumoto, A., McMullen, J. R., Eckle, S. B., Bertolino, P., Sullivan, L. C. & Andrews, D. M. (2019). Multiple receptors converge on H2-Q10 to regulate NK and γδT-cell development. Immunology and Cell Biology, 97 (3), pp.326-339. https://doi.org/10.1111/imcb.12222.

DR DAN ANDREWS (Orcid ID : 0000-0002-5896-7885)

Article type : Original Article

Multiple receptors converge on H2-Q10 to regulate NK and γδT cell development

Katharine J. Goodall[1], Angela Nguyen[1], Aya Matsumoto[2], Julie R. McMullen[2,3,4], Sidonia B. Eckle[5], Patrick Bertolino[6], Lucy C. Sullivan[5] and Daniel M. Andrews[1*]

[1]Department of Immunology and Pathology, Central Clinical School, Monash University, Melbourne, Australia.
[2]Baker Heart and Diabetes Institute, Melbourne, VIC, Australia.
[3]Department of Medicine, Monash University, Clayton, VIC, Australia.
[4]Department of Physiology, Monash University, Clayton, VIC, Australia.
[5]Department of Microbiology and Immunology, University of Melbourne, Peter Doherty Institute for Infection and Immunity, Melbourne, Australia.
[6]Liver Immunology program Centenary Institute, University of Sydney, AW Morrow Gastroenterology and Liver Centre and Royal Prince Alfred Hospital, Sydney, NSW,

*To whom correspondence should be addressed: dan.andrews@monash.edu

Running Title: H2-Q10 is a new ligand for CD8αα

This is the author manuscript accepted for publication and has undergone full peer review but has not been through the copyediting, typesetting, pagination and proofreading process, which may lead to differences between this version and the Version of Record. Please cite this article as doi: 10.1111/imcb.12222

Keywords: Non-classical MHC, Natural Killer cells, gamma delta T cells, CD8 alpha/alpha

ABSTRACT

Class Ib MHC are an extended family of molecules which demonstrate tissue-specific expression and presentation of monomorphic antigens. These characteristics tend to imbue class Ib MHC with unique functions. H2-Q10 is potentially one such molecule in that it is overexpressed in the liver but its immunological function is not known. We have previously shown that H2-Q10 is a ligand for the natural killer cell receptor Ly49C and now, using H2-Q10 deficient mice, we demonstrate that H2-Q10 can also stabilize the expression of Qa-1b. In the absence of H2-Q10 the development and maturation of conventional hepatic NK cells is disrupted. We also provide evidence that H2-Q10 is a new high affinity ligand for CD8$\alpha\alpha$ and controls the development of liver-resident CD8$\alpha\alpha$ $\gamma\delta$T cells. These data demonstrate that H2-Q10 has

multiple roles in the development of immune subsets and identify an overlap of recognition within the class Ib MHC that is likely to be relevant to the regulation of immunity.

INTRODUCTION

The major histocompatibility complex (MHC) plays a central role in the development of the immune system and its activation following infection or neoplastic transformation. There are two types of MHC, class I and class II, which activate T cells belonging to the CD8 and CD4 lineages respectively. The class I MHC family can be further subdivided into class Ia and class Ib molecules. Class Ia MHC are ubiquitously expressed and are highly polymorphic. In contrast, class Ib MHC demonstrate tissue specificity and are less polymorphic than their class Ia counterparts [1, 2]. This is thought to allow them to serve more diverse and specialised functions than their class Ia counterparts, whose primary function is the presentation of intracellular peptides to CD8 T cells [3].

In humans, there are only 3 class Ib MHC and these are termed HLA-E/-F/-G [4]. In contrast, the mouse class Ib MHC has undergone a significant expansion and includes multiple genes allocated to 3 subfamilies, H2-Q/-T/-M [1]. Among these 3 subfamilies the Q genes are thought to be more closely related to class Ia MHC than the T family [1, 5, 6]. These observations are supported by the fact that Q family proteins such as H2-Q7/Qa-2 tend to present peptide repertoires that are more reminiscent of class Ia MHC [7], while the T family molecules such as H2-T10/22 and H2-T3/TL do not [8, 9]. Further separated from the class Ia MHC at the distal end of the MHC-encoding locus

on chromosome 17 in mice, the M family may have evolved from an ancient MHC-like molecule and appears to be largely divergent from class Ia MHC [10].

While these data suggest an interesting role for evolution in the development of the class Ib MHC, there is a significant gap in our understanding of the molecules. This is most easily highlighted by the fact that out of the approximately 30 genes in the mouse class Ib MHC complex, only 7 of these molecules have been examined beyond their pattern of tissue expression [1]. Furthermore, the immunological function of only 4 of these 7 molecules has been explored [11]. This represents a significant lapse in our understanding of these MHC which is particularly relevant given the fact that they represent ligands for specialised and novel immune pathways such as γδT cell restriction (H2-T10/22) [8, 12, 13], CD94/NKG2 interactions (Qa-1b) [14, 15] or CD8αα recognition (H2-T3/TL) [9].

One of the most intriguing class Ib MHC is H2-Q10. This molecule was first identified almost 30 years ago during a sequence analysis of class I MHC clones [16]. This study demonstrated that H2-Q10 lacked a transmembrane region and transcription could only be detected in the liver where it made up 20% of the total MHC pool [16]. Subsequent studies confirmed that H2-Q10 could be secreted with protein detected at high concentrations in the serum [17, 18]. Much like H2-Q7/Qa-2, H2-Q10 was subsequently shown to bind a classical peptide repertoire [19] and we have recently demonstrated that H2-Q10 is able to bind to the natural killer (NK) cell receptor, Ly49C [20]. Despite these observations, the immunological function for H2-Q10 remains unknown.

Using a newly derived H2-Q10 deficient mouse strain, we have made an assessment of the role of this class Ib MHC in the development of liver-specific lymphocytes. Our data provide evidence that H2-Q10 plays a role in the development of liver conventional NK (cNK) and γδT cells, an effect modulated via multiple pathways of recognition. While regulation of cNK is polygamous and involves Qa-1b mediated presentation of the H2-Q10 leader sequence as well as the direct recognition by Ly49C, the interaction with γδT

cells is monogamous and occurs via CD8αα. Therefore, we provide evidence that H2-Q10 is a new, high affinity ligand for CD8αα, an observation that provides a rationale for the presence of CD8αα expressing cells outside of the small intestine. These new data reinforce the role of class Ib MHC as class Ia MHC independent and highly specialised molecules and highlights the need for the ongoing study of these molecules as immune modulators.

RESULTS

The H2-Q10 leader sequence can stabilise Qa-1b

We have previously demonstrated that H2-Q10 binds Ly49C, however this occurs with an affinity lower than that of H-2K^b [20], suggesting that H2-Q10 is unlikely to be the primary recognition element for Ly49C. The leader sequence of H2-Q10 contains Qdm, which is the high affinity peptide occupying the groove in Qa-1b [21] and this could also be a target for lymphocyte recognition. In order to determine whether H2-Q10 regulated the expression of Qa-1b, we generated B16F10 cells expressing H2-Q10 or H2-Q10 in which the leader sequence was substituted with that of H-2K^b (K^{b}Q10), which does not contain Qdm [22]. Overexpression of H2-Q10 in these cells demonstrated an up-regulation of Qa-1b at the cell surface when compared to K^{b}Q10 (**Figure 1a**).

With these data sets in hand, we began exploring the immunological consequences of H2-Q10 deficiency *in vivo*. Whilst it has been shown that H2-Q10 is highly expressed in the liver, it is necessary as a first step to further identify which liver cells are responsible for H2-Q10 expression. As hepatocytes are the principal hepatic cell, we reasoned that H2-Q10 expression would be restricted to these cells. Transcript H2-Q10 expression levels in total liver were equivalent to those in purified hepatocytes, (**Figure 1b**) and significantly enriched (P = 0.0003) when compared to non-hepatocytes **(Figure 1b**), suggesting that hepatocytes were the source of H2-Q10.

To examine whether lack of H2-Q10 expression influenced Qa-1b expression levels, hepatocytes from wild type and H2-Q10 deficient mice were analysed

for the expression of Qa-1b as well as H-2K^b, H-2D^b and H2-Q7/9. While expression of H-2K^b, H-2D^b and H2-Q7/9 was not altered in the absence of H2-Q10, we did observe a significant (P = 0.0003) decrease in the expression of Qa-1b on hepatocytes (**Figure 1c and e**) but not leukocytes (**Figure 1d and e**). Together, these data demonstrate a requirement for the H2-Q10 leader sequence in the surface expression of Qa-1b.

H2-Q10 plays a role in the development of liver cNK

Qa-1b is the ligand for heterodimeric complexes of CD94/NKG2 [15, 22] expressed on a variety of lymphocytes but most commonly associated with NK cells and innate lymphoid cells (ILCs). Having demonstrated a requirement of H2-Q10 for the stabilization of Qa-1b, we next sought to determine whether this interaction could have any effect on the development of NK cells/ILCs as these cells constitutively express CD94 at high levels. As a first step, we examined the development of total NKp46$^+$/CD3$^-$ populations in the spleen and liver.

NKp46$^+$/CD3$^-$ cells are comprised of CD49a$^+$ ILC-1 cells and CD49b$^+$ conventional NK cells (cNK) [23]. In line with the observation that H2-Q10 is not expressed in the spleen [1] we observed no effect of H2-Q10 deficiency on the development of CD49a$^+$ ILC-1 or CD49b$^+$ cNK cells in this organ (**Figure 2a**). In contrast, we observed a significant alteration in the balance of ILC-1 and cNK cells (** P = 0.0017 and 0.0019 respectively) in the livers of H2-Q10 knockout mice, (**Figure 2b**). Wild type mice tended to have a larger proportion of cNK cells compared to ILC-1 while this was reversed in the H2-Q10 deficient mice (**Figure 2b**). While we observed a trend towards a reduction in total NKp46$^+$/CD3$^-$ cells in the liver of H2-Q10$^{-/-}$ mice, this was not significant however we did observe a significant (*P = 0.0499) decrease in the number of cNK cells, (**Figure 2b**). We did not observe any effect of H2-Q10 deficiency on the total number of ILC-1 (**Figure 2b**), an observation we associate with the lower numbers of total NKp46$^+$/CD3$^-$ cells.

Having demonstrated an effect on cNK cell development in H2-Q10-deficient mice, we next analysed the development of subsets within this population.

Using our observations that H2-Q10 is a ligand for Ly49C [20] and stabilizes the CD94 ligand, Qa-1b (**Figure 1**) we assessed the presence of subsets expressing CD94 and Ly49C-I. We were unable to source a Ly49C specific antibody but H2-Q10 does not bind Ly49I [20], suggesting that any effects on the Ly49C-I population will be Ly49I independent. Using these markers allowed us to separate ILC-1 and cNK cells into populations that are immature ($CD94^+/Ly49C^-$) and mature ($CD94^-/Ly49C^+$). Analysis of these populations within the cNK cell pool demonstrated that H2-Q10-deficient mice had a significant increase in the percentage (*P = 0.0407) and number (***P = 0.0002) of $CD94^+/Ly49C\text{-}I^-$ immature populations with a corresponding decrease in the frequency (**P = 0.0019) and number (**P = 0.0070) of $CD94^+/Ly49C\text{-}I^+$ cells, (**Figure 3a**). In contrast, no effect was observed in the ILC populations (**Figure 3b**). Similar to the effects observed for CD94/Ly49C, we also observed significant alterations the populations of NK cells expressing CD27 and CD11b. The absence of H2-Q10 resulted in significant alterations to the frequency and number of $CD27^{\pm}/CD11b^-$ and $CD27^-/CD11b^{\pm}$ NK cell subsets (**Supplementary Figure 1**). Further examination of a panel of additional inhibitory receptors demonstrated no role for H2-Q10 in the expression of KLRG1, CD96 and TIGIT (**Supplementary Figure 1**). These data indicate H2-Q10 plays an important role in the development of liver NK cells and highlights the specificity of the interaction for Qa-1b.

In order to determine whether H2-Q10 deficiency also regulated the function of these cNK cell subsets, we sorted and stimulated them in the presence of IL-12/IL-18 or IL-12/IL-15 to determine their capacity to produce IFN-γ and MIP-1α respectively [24]. These experiments demonstrated no significant difference in IFN-γ (**Figure 3c**) or MIP-1α (**Figure 3d**) production for either the $CD94^+/Ly49C\text{-}I^-$ or the $CD94^-/Ly49CI^+$ populations in wild type and H2-Q10 deficient mice. Similarly, we observed no difference in the cytotoxic capacity of liver NK cells directed against cells expressing ligands for NKG2D or DNAM-1, (**Supplementary Figure 2**). These data demonstrate that H2-Q10 plays a role in the development of cNK cell subsets in the liver but does not affect their functionality.

H2-Q10 plays a role in the development of CD8αα$^+$ γδT cells

CD94/NKG2 heterodimers can be found on other subsets of cells including CD8 T cells, NKT cells and γδT cells. Given our observation regarding H2-Q10, Qa-1b and cNK cells, we next sought to determine whether H2-Q10 played a role in the development of other subsets of lymphocytes found in the liver. Leukocytes from the spleen and livers of wild type and H2-Q10$^{-/-}$ mice were prepared and subsets of CD8, NKT and γδT cells were analysed. A comparison of CD8 and NKT cells demonstrated no significant differences in the number and frequency of these cells in the spleen or liver (**Supplementary Figure 3**). In contrast, a significant decrease (*P = 0.0104) in liver γδT cells was observed in H2-Q10$^{-/-}$ mice (**Figure 4a**). In a similar manner to the ILC and NK cells, we then analysed the populations of CD94 and Ly49C expressing subsets of γδT cells. In contrast to the effects we observed on the NK cells, there was no difference in the CD94/Ly49C-I subpopulations in the γδT cell pool (**Figure 4b**).

Due to the majority of γδT cells not expressing Ly49C-I, this indicated that H2-Q10 may be regulating these cells via an alternative receptor. Therefore, we then other populations of γδT cells and, in particular, we focused on the CD8 subsets as this molecule can also interact with class I MHC. These studies identified a significant decrease in the proportion (~20% in wild type vs ~8% in H2-Q10$^{-/-}$ *P = 0.0407) and number (15034 ± 3520 in wild type vs 4934 ± 656 in H2-Q10$^{-/-}$ ** P = 0.0070) of CD8αα TCRγδ T cells, (**Figure 4c**). This effect was specific for the liver as no differences were observed in the spleen (**Figure 4c**).

The principal ligand for CD8αα, H2-T3/TL, demonstrates restricted expression on intestinal epithelial cells of the small intestine [25, 26] which is also the location of a large population of CD8αα cells [27]. In order to determine whether the effects we were observing we related to altered expression of H2-T3/TL in H2-Q10 deficient mice, we analysed the expression of this gene in hepatocytes. In line with previous data [1, 25, 26], we were unable to detect H2-

T3/TL transcripts in the livers but it was highly expressed in the small intestine, (**Figure 4d**). This indicated that the effects we observed on CD8αα TCRγδ cells were independent of H2-T3/TL. Together, these data demonstrate that H2-Q10 plays a role in the development of γδT cells expressing CD8αα in the liver which is independent of Qa-1b, CD94, Ly49C and H2-T3/TL.

CD8αα γδT cells are liver resident

Under homeostatic conditions, CD8αα cells in the gut are liver-resident [28], suggesting a localisation of these cells at the site of their ligand. This prompted us to determine whether the CD8αα cells in the liver are similarly restricted, which would allow them constant exposure to H2-Q10 produced by hepatocytes. As such, we performed parabiosis studies where pairs of wild type and congenic CD45.1 mice were surgically engrafted and the circulation allowed to mix for a period of 3 weeks. Following this time, we harvested the livers and assessed the residence/circulating capacity of ILC-1, cNK and CD8αα γδT cells. cNK cells were not restricted to the liver as demonstrated by the equal amounts of $CD45.1^+$ and $CD45.2^+$ cells in the CD45.1 and CD45.2 parabionts (**Figure 5a**). In contrast, ILC cells demonstrate a high degree of liver residence with greater than 80% of these cells being of host origin (**Figure 5a**). When we analysed the γδT cell pool, $TCR\gamma\delta^+$ $CD8\alpha\beta^+$ T cells demonstrated a preference to migrate out of the liver as these cells were predominantly enriched for $CD45.2^+$ cells in the CD45.1 parabiont and vice versa (**Figure 5b**). Similar to the ILC-1, $CD8\alpha\alpha^+$ γδT cells largely retained in the liver of their origin (**Figure 5b**). Thus, liver specific expression of H2-Q10 is associated with the retention of CD8αα γδT cells, analogous to the interaction between H2-T3/TL and CD8αα cells in the gut.

H2-Q10 is a high affinity ligand for CD8αα

Finally, our observations regarding CD8αα γδT cells and H2-Q10 prompted us to explore the possibility that H2-Q10 represented a new ligand for CD8αα. To test this hypothesis, we examined the capability of hepatic CD8αα TCRγδ

cells in the liver to bind H2-Q10 and the prototypical CD8αα ligand, H2-T3/TL. Using a FACS based approach, we observed a strong interaction between H2-Q10 and the subset of γδT cells expressing the CD8αα homodimer, which was similar to that observed for H2-T3/TL (**Figure 6a**). In contrast, we did not observe binding to the $CD8^-$ population (**Figure 6a**). In order to confirm that H2-Q10 was binding to CD8αα, we performed direct binding studies using SPR. The results from these experiments reinforced our tetramer data and showed that H2-Q10 bound to CD8αα (**Figure 6b**), with an affinity (~300nM) higher than that of positive control H2-T3/TL (~800nM) (**Figure 6c**). To confirm the interaction between H2-Q10 and CD8αα was occurring in a cellular context we pre-treated γδT cells with CT-CD8a, which has previously been shown to inhibit MHC binding to CD8 [29]. In contrast to the isotype, pre-treatment with CT-CD8a completely impaired H2-Q10 binding to $CD8\alpha\alpha^{\pm}$ γδT cells, (**Figure 6d**). These data identify H2-Q10 as a new high affinity ligand for CD8αα.

DISCUSSION

The large family of genes that comprises the class Ib MHC in the mouse remains underexplored. This is a clear deficit in our understanding of immunity when considering the unique function of class Ib MHC members such as H2-T3/TL, Qa-1b and H2-M3. Our previous results have demonstrated that H2-M3 controls NK cell responses through the inhibitory receptor Ly49A [30] and that H2-Q10 binds to Ly49C [20]. We have now added to this data set by demonstrating that H2-Q10 acts to control the development of lymphocyte subsets found in the liver and performs this function via different receptor-ligand pathways. As such, H2-Q10 appears to simultaneously control NK and γδT cell development in the liver and, therefore, represents the first class I MHC able to act in this manner.

One of the main drivers of the development of the immune system is co-evolution with viruses. Many viruses have developed means by which to orchestrate the immune response such that a non-sterilising response occurs, allowing the virus to persist life-long with its host. Qa-1b recognition by

CD94/NKG2 heterodimers is thought to be an example of a relatively new immune pathway, driven by the co-evolution between the murine immune system and Cytomegalovirus (CMV) [31]. A similar observation can be made with another mouse pathogen, Lymphocytic Choriomeningitis Virus (LCMV) [32]. However, of more relevance here would be the association between H2-Q10 and murine hepatitis virus (MHV), given the fact that H2-Q10 and the infection are highly restricted to the liver. Interestingly, NK cells and γδT cells have both been implicated in the response to MHV [33, 34] and MHV infection is lethal in neonates and weaning mice but is asymptomatic in adults [35]. These results reflect our observations regarding H2-Q10 and the innate immune cells in the liver as well as the expression pattern of H2-Q10, which does not reach high levels in the liver until post-weaning [18]. An investigation of the role of H2-Q10 during MHV infection, while a logistical challenge, would represent an excellent opportunity to assess virus-host co-evolution.

The ability of H2-Q10 to stablise Qa-1b is not unique to this molecule. Indeed, the Qdm peptide can be found in several class I MHC leader sequences, where it acts as a measure of class I MHC bio-synthesis. While our *in vitro* data demonstrated that the leader sequence of H2-Q10 could stabilise Qa-1b expression, we did not observe a complete downregulation of Qa-1b in H2-Q10 deficient hepatocytes. This is most likely due to the fact that H-2D^b also contains the Qdm peptide [36], as does H2-T13/Blastocyst MHC [37] and either of these MHC could be providing a source of Qdm in the absence of H2-Q10. Another target for H2-Q10 derived Qdm could be the Qa-1b paralog, H2-T11. This molecule shares significant homology with Qa-1b and has a high affinity for Qdm peptides to occupy its groove but it is not recognised by CD94/NKG2 complexes or Qa-1b restricted CD8 T cells [38]. The function of H2-T11 is unknown but as it is expressed in the liver [38], a potential interaction with H2-Q10 should be explored.

Another interesting question regarding H2-Q10 and Qa-1b would be the effect of H2-Q10 derived Qdm outside of homeostasis. Under normal conditions, the groove of Qa-1b is largely occupied by Qdm owing to its capacity to

outcompete other peptides [39]. However, this balance can be upset during infections such as *Listeria monocytogenes* [40] and *Salmonella typhimurium* [41]. Interestingly, infection with Salmonella typhimurium can induce a Qa-1b restricted CD8 T cell response against a peptide derived from the GroEL protein (GMQFDRGYL) which cross reacts with a peptide derived from Heat Shock Protein 60 (HSP60) (GMKFDRGYI) [42]. Qa-1b molecules in which the Hsp60 peptide occupies the groove can be found under conditions of stress and these become a target for CTL [42, 43]. Given that hepatocytes are highly secretory cells and are thus rich in Endoplasmic Reticulum, any level of stress could be enough to induce Qa-1b expression in which self-peptides like Hsp60 are presented. Given the importance of the liver in overall health and survival, the generation of liver specific, Qa-1b restricted CD8 T cells would be a significant problem. As such, it is possible that the overexpression of H2-Q10 in this organ helps protect against the generation of autoimmunity by providing a constantly saturating, competitive level of Qdm that is able to reduce or prevent the generation of self-restricted Qa-1b specific T cells.

The absence of H2-Q10 altered the balance of cNK and ILC-1 in the liver and further regulated the maturation of cNK cell subsets, with a propensity for the cells to accumulate at the more immature CD94+/Ly49C-I- stage. Despite this, we did not observe any alterations in cytokine-producing capacity of the cNK cell populations, suggesting that the functionality of these cells remains intact. It was interesting to note that the absence of H2-Q10 did not affect the maturation of ILC-1, given that these cells are liver-restricted while the cNK cells are not (**Figure 5**) [44, 45]. As such, it would be expected that ILC-1 would be more consistently exposed to Qa-1b and the associated reduction of its expression in H2-Q10 deficient mice. This would suggest that ILC-1 are less responsive to minor alterations in the expression of Qa-1b than their cNK counterparts. This does not appear to be due to differences in CD94 and NKG2A/C/E expression as cNK and ILC-1 express equivalent levels of these receptors (**Figure 3**) [46]. Given that H2-Q10 can bind to Ly49C as well as regulate the expression of Qa-1b, it is possible that the absence of H2-Q10 is affecting the cNK cells through both pathways. In support of this, biochemical analysis of H2-Q10 binding to Ly49C demonstrates that H2-Q10 is a low

affinity ligand for this receptor and, in fact, cannot bind this receptor when H-2K^b is present [20]. This would suggest that the predominant pathway by which cNK cell maturation is regulated in H2-Q10 deficient mice is through Qa-1b. However, Qa-1b deficient mice have normal numbers of cNK and ILC-1 in the liver [46]. Given the promiscuity of Ly49C for class I MHC [20, 47, 48] , it remains possible that another, unrecognized class Ib MHC is contributing to the development of Ly49C expressing NK cells and this this interaction involves a contribution from H2-Q10.

The observation that H2-Q10 deficient mice had a defect in CD8αα TCRγδ cells was unexpected, although not completely surprising. Until our observation, the only known ligand for CD8αα is the class Ib MHC, H2-T3/TL [9]. Biologically, H2-T3/TL and CD8αα expressing cells are well matched as both are found in the small intestine, where they demonstrate restricted expression on epithelial cells [25, 26] and residence [28]. Our data regarding H2-Q10 mirrors this interaction as H2-Q10 is overexpressed in hepatocytes and CD8αα TCRγδ cells are resident in the liver. As such, the CD8αα TCRγδ cells in the liver would be exposed to a constant source of H2-Q10, much like the cells in the small intestine and H2-T3/TL. It is important to note that we have also demonstrated that that H2-Q10 binds to CD8αα with an affinity that exceeds that of H2-T3/TL. Thus, in an *in vivo* developmental setting, this suggests that any interaction with CD8αα would favour binding of H2-Q10 over H2-T3/TL. However, we have demonstrated that the absence of H2-Q10 results in a loss of CD8αα TCRγδ cells, while the absence of H2-T3/TL has no effect on CD8αα cell development in the small intestine [49]. Thus, the absence of H2-Q10 should have no effect on the development of CD8αα TCRγδ cells if H2-T3/TL is present, however, we and others have demonstrated [1, 25, 26] that H2-T3/TL is not expressed in the liver. Given that H2-Q10 is a soluble MHC, it is unlikely to directly stimulate CD8αα, suggesting that it acts to inhibit interaction with stimulating receptors, subsequently resulting in cell death. Given that we have identified another class Ib MHC ligand for CD8αα, it remains possible that other members of the class Ib MHC bind this molecule and, in the absence of H2-Q10, induce the death of these cells via low affinity

interactions. Further investigation of the capacity of other class Ib MHC to act in this area should prove useful.

As a corollary to the above, it has been demonstrated that conventional CD8 T cells upregulate CD8αα homodimers shortly after activation and that this controls survival and development of memory [50]. It is possible to induce activated, long lived CD8 T cells in the liver [51] but the dependence on CD8αα has not been explored. Much like its effect on CD8αα TCRγδ cells, it is possible to speculate that H2-Q10 prevents the generation of CD8 T cell memory in the liver by inhibiting the engagement of other, lower affinity molecules. It is not hard to imagine similar interactions occurring in other sites where class Ib MHC are restricted. Targeting these MHC to determine their capacity to bind CD8αα will be an essential first step.

Collectively, our data have demonstrated that H2-Q10 is the focus of multiple receptors and that is plays an essential role in the development of innate lymphocytes. Significant overlap in terms of restricted expression and association with resident lymphocytes demonstrate that H2-Q10 shares some features in common with H2-T3. Further exploration of other, tissue-restricted class Ib MHC will be essential to exploring the unique characteristics of this interesting family of molecules.

METHODS

Mice: C57BL/6 mice were from Alfred Medical Research and Education Precinct (AMREP) Animal services. C57BL/6.H2-Q10$^{tm1.1(KOMP)Mbp}$ mice were generated by the trans-NIH Knock-Out Mouse Project (KOMP) and obtained from the KOMP repository (www.komp.org). NIH grants to Velocigene at Regeneron INC (U01HG004085) and the CSD Consortium (U01HG004080)

funded the generation of gene-targeted ES cells for 8500 genes in the KOMP Program and archived and distributed by the KOMP Repository at UC Davis and CHORI (U42RR024244). A LacZ and Neomycin construct was inserted into the coding region of H2-Q10. Cre recombinase was then used to excise the neomycin gene leaving LacZ in the 2nd exon of H2-Q10, (**Supplementary Figure 4**). A breeding colony of homozygous C57BL/6.H2-Q10$^{tm1.1(KOMP)Mbp}$ knockouts were established at Monash University Animal Services (Clayton). Genotyping of breeding pairs was performed by Transnetyx (Memphis, Tennessee, USA) using real-time PCR (RT-PCR). All mice were used between 6 and 8 weeks of age. All experiments were in accordance with the animal ethics guidelines of the National Health and Medical Research Council of Australia. All experiments were approved by the AMREP Animal Ethics Committee.

Generation of recombinant CD8αα: The sequence of soluble mouse CD8αα, allele CD8A*02, was designed based on a previously published sequence to fold soluble mouse CD8α/CD8β following *E. coli* expression [52], GenBank accession number GQ247790.1, except for the following modifications whereby residue numbering is based on Kern *et al* [52]: (i) Cys36 was mutated to Ser as based on crystal structures of CD8αα, Cys 36 is not involved in disulphide bonds [52, 53] and we suspected that mutating this residue might improve folding efficiency, (ii) the gene was shorted to cover residues $^{-5}$Gly to ^{128}Lys, as in previously determined crystal structures that included mouse CD8αα or CD8αβ there was no data beyond this region, (iii) the gene was codon optimized for E. coli expression by Genscript (Piscataway, NJ, USA). The gene was purchased from Genscript and subcloned into a pET30 expression vector, expressed in BL21 *E.coli* competent cells and purified from inclusion bodies. The inclusion bodies were solubilized in 6M guanidine-HCl and 120 mg/L of total protein (split over 3 injections) was rapidly diluted in a buffer containing 0.4M arginine hydrocholoride, 100 mM Tris-HCl (pH8), 2 mM EDTA, 3 mM reduced glutathione and 0.3 mM oxidized glutathione and allowed to sit for 2-3 days at 4°C. The refold was then dialyzed against 25 mM MES (pH6) overnight, followed by filtration through a 0.45 μM filter. The

CD8αα was purified by cation exchange using Hi-Trap SP column (GE Healthcare, Chicago, Illinois, USA) and eluted using 25 mM MES (pH6) containing 1M NaCl. The major peak was pooled, concentrated and further purified by size exclusion chromatography using Superdex 75 column with a buffer containing 25 mM Hepes (pH 7.4) with 150 mM NaCl.

Generation of tetramers: cDNA encoding residues 20-274 of H2-Q10 and H2-T3/TL were generated by Genscript and cloned into a pUC57 vector. These were sub-cloned into a pET-30-based vector that allowed for an in-frame fusion of a substrate peptide for the enzyme BirA. The heavy chains of H2-Q10, TL and mouse β2-microglobulin were expressed separately in *E. coli,* purified from inclusion bodies and refolded in the absence of peptide (H2-T3/TL) or in the presence of ribophorin (VGITNVDL) for H2-Q10.

Generation of B16F10-Q10 cell lines: The full length sequences of wild type and Qdm mutated H2-Q10 were cloned into the MSCV plasmid and retroviral supernatants generated using 293T cells. B16F10 cells infected with retrovirus were sorted on the basis of GFP expression. Populations were sorted until stable with insertion of the class Ib MHC determined by PCR (H2-Q10).

Real-time PCR (RT-PCR): Total RNA was isolated from cells either using the RNEasy kit (Qiagen, Venlo, The Netherlands), or TRI Reagent RT (Merck, Darmstadt, Germany) and complementary DNA (cDNA) synthesized from 1 µg total RNA using an iScript cDNA Synthesis Kit (Bio-Rad, CA, USA). Complementary DNA was amplified using QuantiNova SYBR Green mix (Qiagen) and the Quantstudio 6 qPCR (Applied Biosystems, Foster City, USA) with a two-step protocol including an annealing/extension temperature of 60°C for all primer pairs. Primer sequences are shown in Supplementary Table 1.

Flow Cytometry.

Flow cytometric analysis of organs: Organs were collected from wild type and H2-Q10 deficient mice and single cell suspensions prepared using standard protocols [30]. Following removal of red blood cells using ACK, nonspecific receptors were blocked with monoclonal antibody (mAb) 2.4G2, then cells (5 x 10^6) were stained with mAb to H-2K^b (AF6-88.5; Biolegend, San Diego, CA, 92121, USA), H-2D^b (KH95; Biolegend), H2-Q7/9 (695H1-9-9; Biolegend), NKp46 (29A1.4; Biolegend), CD49a (HMα1; Biolegend), CD49b (HMα2; Biolegend), CD94 (18d3; Biolegend), Ly49C/I (14B11; BD Biosciences), TCR$\gamma\delta$ (GL3; Biolegend), TCRβ (H57-597; Biolegend), CD3 (17A2; Biolegend), CD8α (53-6.72; Biolegend and CT-CD8a ThermoFisher Scientific, Waltham, MA, USA), CD8β (53-5.8; Biolegend), CD27 (LG.3A10; Biolegend), CD11b (M1/70; Biolegend), KLRG1 (2F1/KLRG1; Biolegend), CD96 (3.3; Biolegend), TIGIT (1G9; Biolegend) and tetramers. Cells stained with tetramers were fixed in 2% paraformaldehyde, washed twice in PBS before being resuspended in FACS buffer (PBS-1%FCS). All other flow cytometry combinations were acquired unfixed. For acquisition, events were electronically gated on FSC-A vs FSC-H (singlets), followed by FSC-A and SSC-A (to exclude doublets and debris). Among the remaining population at least 5000 electronic events of interest were collected using an LSR-II or X-20 Fortessa (BD Biosciences, Franklin Lakes, NJ, 07097, USA).

Flow cytometric analysis of B16F10 cells: B16F10-Q10 cells were incubated in the presence of recombinant IFN-γ (Biolegend, 100U/mL^{-1}) for 2 days and then blocked with 2.4G2 prior to staining with Qa-1b antibody (6A8.6F10.1A6; BD Biosciences). For acquisition, events were electronically gated on FSC-A vs FSC-H (singlets), followed by FSC-A and SSC-A (to exclude doublets and debris). Among the remaining population at least 10000 electronic events of interest were collected using an LSR-II (BD Biosciences).

Sorting of Liver populations into hepatocyte and non-hepatocyte populations: Livers were perfused with ice cold PBS and dissected whole. They were subsequently dissociated in the presence of 100U/ mL^{-1} Collagenase at 37 degrees for 30 minutes. Single cell suspensions were then filtered through

100μM and centrifuged twice using ice cold PBS. Hepatocytes and non-hepatocytes were subsequently sorted on the basis of size and complexity (FSC^{hi} v SSC^{hi} for Hepatocytes and FSC^{lo} v SSC$^{lo/hi}$ for non-hepatocytes **Supplementary Figure 5**).

Preparation of small intestine: Intestinal epithelial cells were purified as described [54].

Sorting, activation and intracellular detection of IFN-γ in cNK: cNK cells were sorted using a FACSAria (BD Biosciences). 2 x 10^5 cells were sorted/well and triplicate cultures were setup in the presence of 1ng/ mL^{-1} IL-12 and 5ng/ mL^{-1} IL-18 or 1ng/ mL^{-1} IL-12 and 50ng/ mL^{-1} IL-15 [24]. After 6 and 24h of incubation, supernatant was removed and the presence of IFN-γ determined using a Cytometric Bead Array (CBA) (BD Biosciences), following the manufacturers protocol.

Cytotoxicity assays: NK cells were sorted on a FACSAria (BD Biosciences) and co-cultured with YAC-1 (NKG2D ligands) or B16F10 (DNAM-1 ligands) at different ratios. Cytotoxicity was determined using the 51Cr assay as previously described [55].

Surface Plasmon Resonance. Surface plasmon resonance (SPR) was performed essentially as described [20]. Briefly, biotinylated MHC were captured on the surface of a ProteOn NLC neutravidin chip (Bio-Rad, ~150 RU of each). An empty flow cell with neutravidin alone served as a control. Serially diluted CD8αα, produced as described above was injected simultaneously over the control and test surfaces. After subtraction of data from the control flow cell, K_D was calculated by kinetic analysis using a Langmuir 1:1 binding model with the ProteOn Manager software (Bio-Rad).

Parabiotic mice. Parabiosis surgery was performed as previously described [56]. Briefly, pairs of female C57BL/6 and B6.SJL-*Ptprc*^{a} *Pepc*^{b}/BoyJ mice, of equal weight, were acclimatised for a period of 2 weeks prior to surgery. Pairs that

demonstrated harmonious cohabitation were then supplied with antibiotics (Bactrim containing Sulfamethoxazole, 2 mg/ mL^{-1} and Trimethoprim, 0.4 mg/ mL^{-1}) ad libitum in the drinking water for the 3-day period leading up to surgery up until 10 days after surgery. Prior to surgery, mice were treated with Carprofen (10mg/kg s.c.) and Buprenorphine (0.1mg/kg s.c.). The anaesthetic plane was induced with 4-5% Isoflurane. Anaesthesia was maintained with 2% Isoflurane and mice were shaved along opposite lateral flanks. The skin was then wiped with alcohol and Betadine wipes before mirrored, longitudinal incisions were made along the lateral aspect of each mouse. Joining of the mice was initiated by attaching the olecranon/elbow and the knee joints using non-absorbable 3-0 nylon suture. Following the attachment of the joints, the skin of two mice was connected with a continuous absorbable 5-0 polyglycolic acid suture starting ventrally from the elbow towards the knee and continued the suture dorsally closed with a surgical double knot. Pairs of mice were allowed to recover for a period of 2 weeks, when a tail vein bleed was performed to confirm parabiosis. 1 week later, confirmed pairs were euthanized and organs prepared for flow cytometry as described above.

Statistical Analysis: The nonparametric, two-tailed Mann-Whitney *U*-test was used to determine the statistical significance of data sets. *P* values of less than 0.05 were considered significant.

CONFLICT OF INTEREST

The authors declare no conflicts

ACKNOWLEDGEMENTS

This work was supported by an NHMRC project grant for DMA and LCS and a Career Development Fellowship (CDF) for DMA. KG was supported by a Monash University Post-Doctoral Award. We thank the members of the Alfred Medical Research and Education Precinct (AMREP) Flow Cytometry unit for expert assistance. We also thank Mrs Debbie Ramsay for assistance with the parabiosis surgeries and the Monash Animal Research Platform (MARP) and AMREP Animal Services (AAS) for husbandry.

AUTHOR CONTRIBUTIONS

KJG and AN designed the experiments and performed them in the laboratory of DMA. The parabiosis studies were performed by AM and JRMcM. SBE produced the recombinant CD8 used in Figure 6. PB provided input regarding experiments. LCS performed the SPR studies and provided intellectual input and helped drive the project. DMA conceived of the project and supervised KJG and AN.

Figure 1: The H2-Q10 leader sequence contains the Qdm peptide of Qa-1b and stabilizes its expression on hepatocytes. (**a**) B16F10 cells stably transfected with full length H2-Q10 (B16F10-Q10) or B16F10 encoding the non Qdm containing leader sequence from H-2K^b (B16F10-K^{b}Q10) were

665 treated with recombinant interferon gamma and the expression of Qa-1b
666 determined by FACS. Histograms are representative of 2 independent
667 experiments performed in triplicate. The control is isotype stained. (**b**) Real
668 time PCR detection demonstrates that H2-Q10 is expressed by hepatocytes
669 and not liver leukocytes. Data are from 6 samples prepared in isolation. *** *P*
670 = 0.0003. Expression of H-2K^{b}, H-2D^{b}, H-2Q7/9 and Qa-1b in hepatocytes (**c**)
671 and splenocytes (**d**) isolated from wild type and H2-Q10 deficient mice. The
672 filled histogram at the base is the unstained control, the middle dark shaded
673 histogram is the expression on wild type hepatocytes while the top light
674 shaded histogram is staining on H2-Q10 deficient hepatocytes. The
675 histograms are representative of 2 independent experiments using 4 mice per
676 experiment (N=8). The numbers in the histogram represent the average
677 median fluorescent intensity. All histograms have been offset and are
678 modal. The controls are isotype stained. (e) Median Fluorescent Intensity
679 (MFI) of Qa-1b expression in Hepatocytes and Splenocytes. Data are pooled
680 from 2 independent experiments using 4 mice per time point (N=8).
681
682
683
684
685
686 **Figure 2: H2-Q10 plays a role in the development of cNK cells in the**
687 **liver.** (**a**) Representative contour plots showing total ILC (NKp46^{+}/CD3^{-}) and
688 the subsets of cNK (NKp46^{+}/CD3^{-}/CD49b^{+}) and ILC-1 (NKp46^{+}/CD3^{-}/CD49a^{+})
689 in the spleen of wild type and H2-Q10 deficient mice. Contour plots are
690 representative of 2 independent experiments using 4 mice per experiment
691 (N=8). The numbers in the plots are the average frequencies from the 8
692 samples (N=8). The absolute number and frequencies of total ILC
693 (NKp46^{+}/CD3^{-}) cNK (NKp46^{+}/CD3^{-}/CD49b^{+}) and ILC-1 (NKp46^{+}/CD3^{-}
694 /CD49a^{+}) in the spleen of wild type and H2-Q10 deficient mice. Data are
695 pooled from 2 independent experiments using 4 mice per experiment (N=8).
696 Note that the y axis is logarithmic for absolute numbers. (**b**) Representative
697 contour plots showing total ILC (NKp46^{+}/CD3^{-}) and the subsets of cNK
698 (NKp46^{+}/CD3^{-}/CD49b^{+}) and ILC-1 (NKp46^{+}/CD3^{-}/CD49a^{+}) in the liver of wild

type and H2-Q10 deficient mice. Contour plots are representative of 2 independent experiments using 4 mice per experiment (N=8). The numbers in the plots are the average frequencies from the 8 samples (N=8). The absolute number and frequencies of total ILC (NKp46$^+$/CD3$^-$) cNK (NKp46$^+$/CD3$^-$/CD49b$^+$) and ILC-1 (NKp46$^+$/CD3$^-$/CD49a$^+$) in the liver of wild type and H2-Q10 deficient mice. Data are pooled from 2 independent experiments using 4 mice per experiment (N=8). * P=0.0499, ** P= 0.0019 for CD49b$^+$ frequency and 0.0017 for CD49a$^+$ frequency. Note that the y axis is logarithmic for absolute numbers.

Figure 3: The absence of H2-Q10 does not affect the maturations and activation of liver cNK cells. (**a**) Representative contour plots showing populations of CD94 and Ly49C-I expressing subsets of cNK in the liver of wild type and H2-Q10 deficient mice. Contour plots are representative of 2 independent experiments using 4 mice per experiment (N=8). The numbers in the plots are the average frequencies from the 8 samples (N=8). The absolute number and frequencies of CD94/Ly49C-I subsets in the cNK population in the liver of wild type and H2-Q10 deficient mice. Data are pooled from 2 independent experiments using 4 mice per experiment (N=8). * P = 0.0407, ** P = 0.0019 for CD94/Ly49C/I frequencies and 0.0070 for CD94/Ly49C/I numbers and *** P = 0.0002. Note that the y axis is logarithmic for absolute numbers. (**b**) Representative contour plots showing populations of CD94 and Ly49C-I expressing subsets of ILC-1 in the liver of wild type and H2-Q10 deficient mice. Contour plots are representative of 2 independent experiments using 4 mice per experiment (N=8). The numbers in the plots are the average frequencies from the 8 samples (N=8). The absolute number and frequencies of CD94/Ly49C-I subsets in the ILC-1 population in the liver of wild type and H2-Q10 deficient mice. Data are pooled from 2 independent experiments using 4 mice per experiment (N=8). Note that the y axis is logarithmic for absolute numbers. cNK cells were purified from the liver of wild type and H2-Q10 deficient mice and the levels of IFN-γ (**c**) and MIP-1α (**d**) determined

following stimulation with IL-12 (1ng/ mL^{-1}) and IL-18 (5ng/ mL^{-1}) (to induce IFN-γ) or IL-12 (1ng/ mL^{-1}) and IL-15 (50ng/ mL^{-1}) (to induce MIP-1α). The results are pooled from 2 independent experiments performed in triplicate (N=6).

Figure 4: H2-Q10 controls the development of CD8$\alpha\alpha$ $\gamma\delta$T cells in the liver. (**a**) Representative contour plots showing total $\gamma\delta$T cells (TCR$\gamma\delta^+$/CD3$^+$) in the spleen and liver of wild type and H2-Q10 deficient mice. Contour plots are representative of 2 independent experiments using 4 mice per experiment (N=8). The numbers in the plots are the average frequencies from the 8 samples (N=8). The absolute number of total $\gamma\delta$T cells (TCR$\gamma\delta^+$/CD3$^+$) in the spleen and liver of wild type and H2-Q10 deficient mice. Data are pooled from 2 independent experiments using 4 mice per experiment (N=8). *P=0.0104. Note that the y axis is logarithmic for absolute numbers. (**b**) Representative contour plots showing CD94 and Ly49C-I expressing $\gamma\delta$T cells in the spleen and liver of wild type and H2-Q10 deficient mice. Contour plots are representative of 2 independent experiments using 4 mice per experiment (N=8). The numbers in the plots are the average frequencies from the 8 samples (N=8). The absolute number of CD94 and Ly49C-I expressing $\gamma\delta$T cells (TCR$\gamma\delta^+$/CD3$^+$) in the spleen and liver of wild type and H2-Q10 deficient mice. Data are pooled from 2 independent experiments using 4 mice per experiment (N=8). Note that the y axis is logarithmic for absolute numbers. (**c**) Representative contour plots showing CD8$\alpha\alpha$ and CD8$\alpha\beta$ expressing $\gamma\delta$T cells in the spleen and liver of wild type and H2-Q10 deficient mice. Contour plots are representative of 2 independent experiments using 4 mice per experiment (N=8). The numbers in the plots are the average frequencies from the 8 samples (N=8). * P = 0.0407. The absolute number of CD8$\alpha\alpha$ and CD8$\alpha\beta$ expressing $\gamma\delta$T cells (TCR$\gamma\delta^+$/CD3$^+$) in the spleen and liver of wild type and H2-Q10 deficient mice. Data are pooled from 2 independent experiments using 4 mice per experiment (N=8). ** P = 0.0070. Note that the y axis is logarithmic for absolute numbers. (**d**) Real time PCR detection demonstrates that H2-T3 is not expressed by hepatocytes but is found in the small intestine (SI). Data are from 4 samples prepared in isolation.

Figure 5: CD8αα cells are resident in the liver. (**a**) Representative contour plots demonstrate electronically gated CD45.1$^+$ and CD45.2$^+$ cells within the ILC populations in the liver. The colors on the chart demonstrate matched congenic markers (blue and black) and mismatched congenic markers (red and green). The corresponding colours are then used to demonstrate the migratory or residence pattern of the subsets as a percentage of distribution (right hand side panel). The green (migratory cNK) and black (resident cNK) panels demonstrate equal mixing while the black (migratory ILC-1) and blue (resident ILC-1) panels demonstrate retention of the ILC-1 in their host. (**b**) Representative contour plots demonstrate electronically gated CD45.1$^+$ and CD45.2$^+$ cells within the CD8αα and CD8αβ subsets of γδT cells populations in the liver. The colors on the chart demonstrate matched congenic markers

(blue and black) and mismatched congenic markers (red and green). The corresponding colours are then used to demonstrate the migratory or residence pattern of the subsets as a percentage of distribution (right hand side panel). The green (migratory CD8$\alpha\beta^+$ TCR$\gamma\delta^+$) and black (resident CD8$\alpha\beta^+$ TCR$\gamma\delta^+$) panels demonstrate a tendency for migration of CD8$\alpha\beta^+$ TCR$\gamma\delta^+$ cells while the black (migratory CD8$\alpha\alpha^+$ TCR$\gamma\delta^+$) and blue (resident CD8$\alpha\alpha^+$ TCR$\gamma\delta^+$) panels demonstrate retention of the CD8$\alpha\alpha^+$ TCR$\gamma\delta^+$ in their host. Data are representative of 2 independent experiments using 3 or 4 pairs of mice per experiment (N=7 pairs).

Figure 6: H2-Q10 is a high affinity ligand for CD8$\alpha\alpha$. (**a**) Representative FACS plots demonstrating binding of H2-Q10 and H2-T3/TL to CD8$\alpha\alpha$ expressing $\gamma\delta$T cells. Cells were electronically gated as TCR$\gamma\delta^+$/CD3$^+$/CD8α^+/CD8β^-. Contour plots are representative of 2 independent experiments using 4 mice per experiment (N=8) and the numbers in the plots are the mean of the 2 experiments (N=8). The raw values for the percent CD8$\alpha\alpha^+$/Tetramer$^+$ events are presented in the chart. Binding of decreasing concentrations of CD8$\alpha\alpha$ (4000, 1600, 640, 256 and 102.4 nM; solid lines, top to bottom) to neutravidin-immobilised H2-Q10 refolded with VGITNVDL (**b**) or H2-TL (no peptide) (**c**); results are presented in response units (RU) after subtraction of baseline values. Plots are representative of at least 2 independent experiments. Dotted vertical lines at 0s indicate injection start. Irregular lines represent raw data and solid lines indicate data fit using a 1:1 Langmuir binding model. (**d**) Pre-treatment with blocking antibody (CT-CD8a) prevents the binding of H2-Q10 tetramers to CD8$\alpha^{\pm}$ $\gamma\delta$T cells. Contour plots are representative of 2 independent experiments using 3 mice per experiment (N=6). The numbers in the plots are the average frequencies from the 6 samples (N=6).

Supplementary Figure 1: H2-Q10 plays a role in liver NK cell development and has no effect on KLRG1, CD96 and TIGIT. (**a**) Representative contour plots showing populations of CD27 and CD11b expressing subsets of cNK in the liver of wild type and H2-Q10 deficient mice. Contour plots are representative of 2 independent experiments using 4 mice per experiment (N=8). The numbers in the plots are the average frequencies from the 8 samples (N=8). The absolute number and frequencies of CD27/CD11b subsets in the cNK population in the liver of wild type and H2-Q10 deficient mice. Data are pooled from 2 independent experiments using 4 mice per experiment (N=8). *** P = 0.0002 for $CD27^{\pm}/CD11b^{-}$ and $CD27^{-}/CD11b^{\pm}$ frequencies and ** P = 0.0070 and 0.0019 for $CD27^{\pm}/CD11b^{\pm}$ and $CD27^{-}/CD11b^{\pm}$ numbers respectively. Note that the y axis is logarithmic for absolute numbers. (**b**) Expression of KLRG1, CD96 and TIGIT on NK cells isolated from the livers of wild type and H2-Q10 deficient mice. The filled histogram at the base is the isotype control, the middle dark shaded histogram is the expression on wild type NK cells while the top light shaded histogram is staining on H2-Q10 NK cells. The histograms are representative of 2 independent experiments using 4 mice per experiment (N=8).

Supplementary Figure 2: The absence of H2-Q10 has no effect on cytotoxicity directed against NKG2D (YAC-1) or DNAM-1 (B16F10). NK cells purified from the liver of wild type and H2-Q10 deficient mice were directly used as effectors in cytotoxicity assays. Decreasing ratios of effectors

and targets co-cultured for 4 hours and the specific lysis determined by ^{51}Cr release.

Supplementary Figure 3: αβ CD8 T and NKT cells develop normally in H2-Q10$^{-/-}$ mice. Leukocytes from the liver of C57BL/6 and C57BL/6.H2-Q10$^{-/-}$ mice were FACS stained to determine the effect of H2-Q10 deficiency on αβ CD8 T and NKT cells. (**a**) Contour plots are representative of 2 independent experiments using 4 mice per time point (N=8). Numbers in the contour plots represent the mean of the 3 experiments (N=8). (**b**) Absolute numbers of αβ CD8 T and NKT cells in C57BL/6 and C57BL/6.H2-Q10$^{-/-}$ mice. Data are pooled from 2 independent experiments using 4 mice per time point (N=8).

Supplementary Figure 4: Generation and validation of H2-Q10 deficient mice. (**a**) Diagrammatic representation of the molecular targeting approach used to disrupt gene expression. H2-Q10 was disrupted following insertion of a LacZ neomycin cassette. Mice with the targeted insert were bred to a Cre delete strain to excise neomycin. As such, exon 2 of the H2-Q10 gene is disrupted by the genomic insertion of LacZ. (**b**) RNA from hepatocytes of wild and H2-Q10 deficient mice was reverse transcribed and used as a template for PCR using primers specific for GAPDH and H2-Q10.

Supplementary Figure 5: Gating strategy for the sorting of hepatocytes and non-hepatocytes from livers. Single cell preparations from enzymatically disrupted livers were sorted for hepatocytes (FSC^{hi} v SSC^{hi}) and non-hepatocytes (FSC^{lo} v SSC^{lo}). Contour plots are representative of 3 independent sorts.

REFERENCES

1. Ohtsuka M, Inoko H, Kulski JK*, et al.* Major histocompatibility complex (mhc) class ib gene duplications, organization and expression patterns in mouse strain c57bl/6. BMC genomics. 2008;**9**:178.

2. Wei XH, Orr HT. Differential expression of hla-e, hla-f, and hla-g transcripts in human tissue. Human immunology. 1990;**29**:131-142.

3. Rossjohn J, Gras S, Miles JJ*, et al.* T cell antigen receptor recognition of antigen-presenting molecules. Annual review of immunology. 2015;**33**:169-200.

4. O'Callaghan CA, Bell JI. Structure and function of the human mhc class ib molecules hla-e, hla-f and hla-g. Immunol Rev. 1998;**163**:129-138.

5. Hughes AL, Nei M. Evolution of the major histocompatibility complex: Independent origin of nonclassical class i genes in different groups of mammals. Mol Biol Evol. 1989;**6**:559-579.

6. Obata Y, Satta Y, Moriwaki K*, et al.* Structure, function, and evolution of mouse tl genes, nonclassical class i genes of the major histocompatibility complex. Proc Natl Acad Sci U S A. 1994;**91**:6589-6593.

7. He X, Tabaczewski P, Ho J*, et al.* Promiscuous antigen presentation by the nonclassical mhc ib qa-2 is enabled by a shallow, hydrophobic groove and self-stabilized peptide conformation. Structure. 2001;**9**:1213-1224.

8. Crowley MP, Reich Z, Mavaddat N*, et al.* The recognition of the nonclassical major histocompatibility complex (mhc) class i molecule, t10, by the gammadelta t cell, g8. J Exp Med. 1997;**185**:1223-1230.
9. Leishman AJ, Naidenko OV, Attinger A*, et al.* T cell responses modulated through interaction between cd8alphaalpha and the nonclassical mhc class i molecule, tl. Science. 2001;**294**:1936-1939.
10. Doyle CK, Davis BK, Cook RG*, et al.* Hyperconservation of the n-formyl peptide binding site of m3: Evidence that m3 is an old eutherian molecule with conserved recognition of a pathogen-associated molecular pattern. Journal of immunology. 2003;**171**:836-844.
11. Goodall KJ, Nguyen A, Sullivan LC*, et al.* The expanding role of murine class ib mhc in the development and activation of natural killer cells. Mol Immunol. 2018e-pub ahead of print May 19;10.1016/j.molimm.2018.05.001.
12. Ito K, Van Kaer L, Bonneville M*, et al.* Recognition of the product of a novel mhc tl region gene (27b) by a mouse gamma delta t cell receptor. Cell. 1990;**62**:549-561.
13. Wingren C, Crowley MP, Degano M*, et al.* Crystal structure of a gammadelta t cell receptor ligand t22: A truncated mhc-like fold. Science. 2000;**287**:310-314.
14. Braud VM, Allan DS, O'Callaghan CA*, et al.* Hla-e binds to natural killer cell receptors cd94/nkg2a, b and c. Nature. 1998;**391**:795-799.
15. Vance RE, Jamieson AM, Raulet DH. Recognition of the class ib molecule qa-1(b) by putative activating receptors cd94/nkg2c and cd94/nkg2e on mouse natural killer cells. J Exp Med. 1999;**190**:1801-1812.
16. Cosman D, Kress M, Khoury G*, et al.* Tissue-specific expression of an unusual h-2 (class i)-related gene. Proc Natl Acad Sci U S A. 1982;**79**:4947-4951.
17. Kress M, Cosman D, Khoury G*, et al.* Secretion of a transplantation-related antigen. Cell. 1983;**34**:189-196.
18. Lew AM, Maloy WL, Coligan JE. Characteristics of the expression of the murine soluble class i molecule (q10). Journal of immunology. 1986;**136**:254-258.
19. Zappacosta F, Tabaczewski P, Parker KC*, et al.* The murine liver-specific nonclassical mhc class i molecule q10 binds a classical peptide

repertoire. Journal of immunology. 2000;**164**:1906-1915.
20. Sullivan LC, Berry R, Sosnin N*, et al.* Recognition of the mhc class ib molecule h2-q10 by the natural killer cell receptor ly49c. J Biol Chem. 2016e-pub ahead of print Jul 6;10.1074/jbc.M116.737130.
21. Zeng L, Sullivan LC, Vivian JP*, et al.* A structural basis for antigen presentation by the mhc class ib molecule, qa-1b. Journal of immunology. 2012;**188**:302-310.
22. Vance RE, Kraft JR, Altman JD*, et al.* Mouse cd94/nkg2a is a natural killer cell receptor for the nonclassical major histocompatibility complex (mhc) class i molecule qa-1(b). J Exp Med. 1998;**188**:1841-1848.
23. Jiao Y, Huntington ND, Belz GT*, et al.* Type 1 innate lymphoid cell biology: Lessons learnt from natural killer cells. Front Immunol. 2016;**7**:426.
24. Baschuk N, Wang N, Watt SV*, et al.* Nk cell intrinsic regulation of mip-1alpha by granzyme m. Cell Death Dis. 2014;**5**:e1115.
25. Hershberg R, Eghtesady P, Sydora B*, et al.* Expression of the thymus leukemia antigen in mouse intestinal epithelium. Proc Natl Acad Sci U S A. 1990;**87**:9727-9731.
26. Wu M, van Kaer L, Itohara S*, et al.* Highly restricted expression of the thymus leukemia antigens on intestinal epithelial cells. J Exp Med. 1991;**174**:213-218.
27. Guy-Grand D, Cerf-Bensussan N, Malissen B*, et al.* Two gut intraepithelial cd8+ lymphocyte populations with different t cell receptors: A role for the gut epithelium in t cell differentiation. J Exp Med. 1991;**173**:471-481.
28. Sugahara S, Shimizu T, Yoshida Y*, et al.* Extrathymic derivation of gut lymphocytes in parabiotic mice. Immunology. 1999;**96**:57-65.
29. Daniels MA, Devine L, Miller JD*, et al.* Cd8 binding to mhc class i molecules is influenced by t cell maturation and glycosylation. Immunity. 2001;**15**:1051-1061.
30. Andrews DM, Sullivan LC, Baschuk N*, et al.* Recognition of the nonclassical mhc class i molecule h2-m3 by the receptor ly49a regulates the licensing and activation of nk cells. Nature immunology. 2012;**13**:1171-1177.
31. Babic M, Krmpotic A, Jonjic S. All is fair in virus-host interactions: Nk cells and cytomegalovirus. Trends Mol Med. 2011;**17**:677-685.

1068 32. Zhou X, Ramachandran S, Mann M*, et al.* Role of lymphocytic
1069 choriomeningitis virus (lcmv) in understanding viral immunology: Past, present
1070 and future. Viruses. 2012;**4**:2650-2669.
1071 33. Khanolkar A, Hartwig SM, Haag BA*, et al.* Protective and pathologic
1072 roles of the immune response to mouse hepatitis virus type 1: Implications for
1073 severe acute respiratory syndrome. J Virol. 2009;**83**:9258-9272.
1074 34. Wu D, Yan WM, Wang HW*, et al.* Gammadelta t cells contribute to the
1075 outcome of murine fulminant viral hepatitis via effector cytokines tnf-alpha and
1076 ifn-gamma. Curr Med Sci. 2018;**38**:648-655.
1077 35. Homberger FR. Enterotropic mouse hepatitis virus. Lab Anim.
1078 1997;**31**:97-115.
1079 36. Kraft JR, Vance RE, Pohl J*, et al.* Analysis of qa-1(b) peptide binding
1080 specificity and the capacity of cd94/nkg2a to discriminate between qa-1-
1081 peptide complexes. J Exp Med. 2000;**192**:613-624.
1082 37. Tajima A, Tanaka T, Ebata T*, et al.* Blastocyst mhc, a putative murine
1083 homologue of hla-g, protects tap-deficient tumor cells from natural killer cell-
1084 mediated rejection in vivo. Journal of immunology. 2003;**171**:1715-1721.
1085 38. Chen L, Reyes-Vargas E, Dai H*, et al.* Expression of the mouse mhc
1086 class ib h2-t11 gene product, a paralog of h2-t23 (qa-1) with shared peptide-
1087 binding specificity. Journal of immunology. 2014;**193**:1427-1439.
1088 39. Kurepa Z, Hasemann CA, Forman J. Qa-1b binds conserved class i
1089 leader peptides derived from several mammalian species. J Exp Med.
1090 1998;**188**:973-978.
1091 40. Bouwer HG, Lindahl KF, Baldridge JR*, et al.* An h2-t mhc class ib
1092 molecule presents listeria monocytogenes-derived antigen to immune cd8+
1093 cytotoxic t cells. Journal of immunology. 1994;**152**:5352-5360.
1094 41. Lo WF, Ong H, Metcalf ES*, et al.* T cell responses to gram-negative
1095 intracellular bacterial pathogens: A role for cd8+ t cells in immunity to
1096 salmonella infection and the involvement of mhc class ib molecules. Journal
1097 of immunology. 1999;**162**:5398-5406.
1098 42. Lo WF, Woods AS, DeCloux A*, et al.* Molecular mimicry mediated by
1099 mhc class ib molecules after infection with gram-negative pathogens. Nat
1100 Med. 2000;**6**:215-218.
1101 43. Davies A, Kalb S, Liang B*, et al.* A peptide from heat shock protein 60

1102 is the dominant peptide bound to qa-1 in the absence of the mhc class ia
1103 leader sequence peptide qdm. Journal of immunology. 2003;**170**:5027-5033.
1104 44. Tang L, Peng H, Zhou J*, et al.* Differential phenotypic and functional
1105 properties of liver-resident nk cells and mucosal ilc1s. J Autoimmun.
1106 2016;**67**:29-35.
1107 45. Weizman OE, Adams NM, Schuster IS*, et al.* Ilc1 confer early host
1108 protection at initial sites of viral infection. Cell. 2017;**171**:795-808 e712.
1109 46. Xu HC, Huang J, Pandyra AA*, et al.* Lymphocytes negatively regulate
1110 nk cell activity via qa-1b following viral infection. Cell Rep. 2017;**21**:2528-
1111 2540.
1112 47. Hanke T, Takizawa H, McMahon CW*, et al.* Direct assessment of mhc
1113 class i binding by seven ly49 inhibitory nk cell receptors. Immunity.
1114 1999;**11**:67-77.
1115 48. Scarpellino L, Oeschger F, Guillaume P*, et al.* Interactions of ly49
1116 family receptors with mhc class i ligands in trans and cis. Journal of
1117 immunology. 2007;**178**:1277-1284.
1118 49. Olivares-Villagomez D, Mendez-Fernandez YV, Parekh VV*, et al.*
1119 Thymus leukemia antigen controls intraepithelial lymphocyte function and
1120 inflammatory bowel disease. Proc Natl Acad Sci U S A. 2008;**105**:17931-
1121 17936.
1122 50. Madakamutil LT, Christen U, Lena CJ*, et al.* Cd8alphaalpha-mediated
1123 survival and differentiation of cd8 memory t cell precursors. Science.
1124 2004;**304**:590-593.
1125 51. Tay SS, Wong YC, McDonald DM*, et al.* Antigen expression level
1126 threshold tunes the fate of cd8 t cells during primary hepatic immune
1127 responses. Proc Natl Acad Sci U S A. 2014;**111**:E2540-2549.
1128 52. Kern P, Hussey RE, Spoerl R*, et al.* Expression, purification, and
1129 functional analysis of murine ectodomain fragments of cd8alphaalpha and
1130 cd8alphabeta dimers. J Biol Chem. 1999;**274**:27237-27243.
1131 53. Kern PS, Teng MK, Smolyar A*, et al.* Structural basis of cd8 coreceptor
1132 function revealed by crystallographic analysis of a murine cd8alphaalpha
1133 ectodomain fragment in complex with h-2kb. Immunity. 1998;**9**:519-530.
1134 54. Graves CL, Harden SW, LaPato M*, et al.* A method for high purity
1135 intestinal epithelial cell culture from adult human and murine tissues for the

investigation of innate immune function. J Immunol Methods. 2014;**414**:20-31.
55. Chan CJ, Andrews DM, McLaughlin NM*, et al.* Dnam-1/cd155 interactions promote cytokine and nk cell-mediated suppression of poorly immunogenic melanoma metastases. Journal of immunology. 2010;**184**:902-911.
56. Kamran P, Sereti KI, Zhao P*, et al.* Parabiosis in mice: A detailed protocol. J Vis Exp. 2013e-pub ahead of print Oct 6;10.3791/50556.

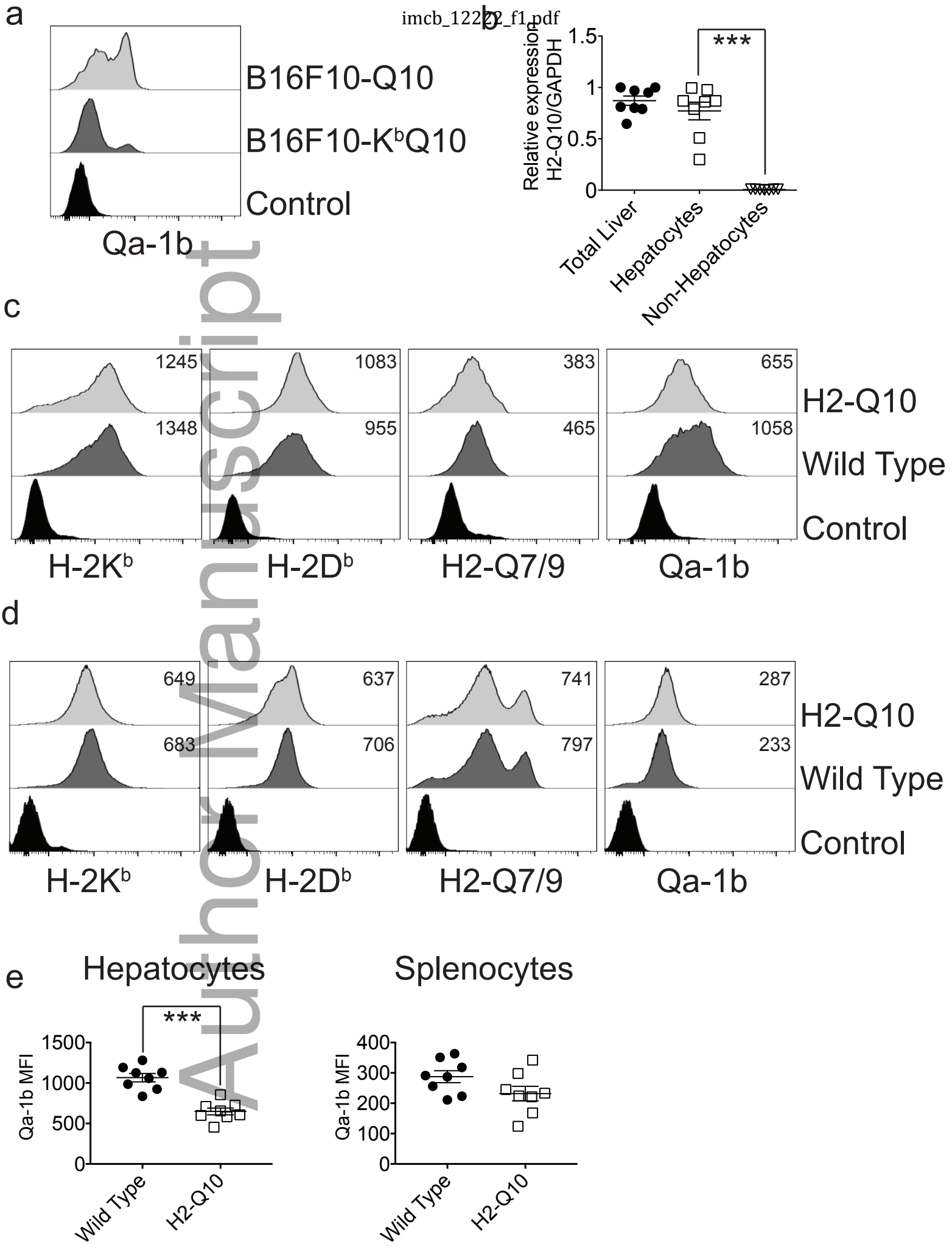

Figure 1 Goodall et al H2-Q10

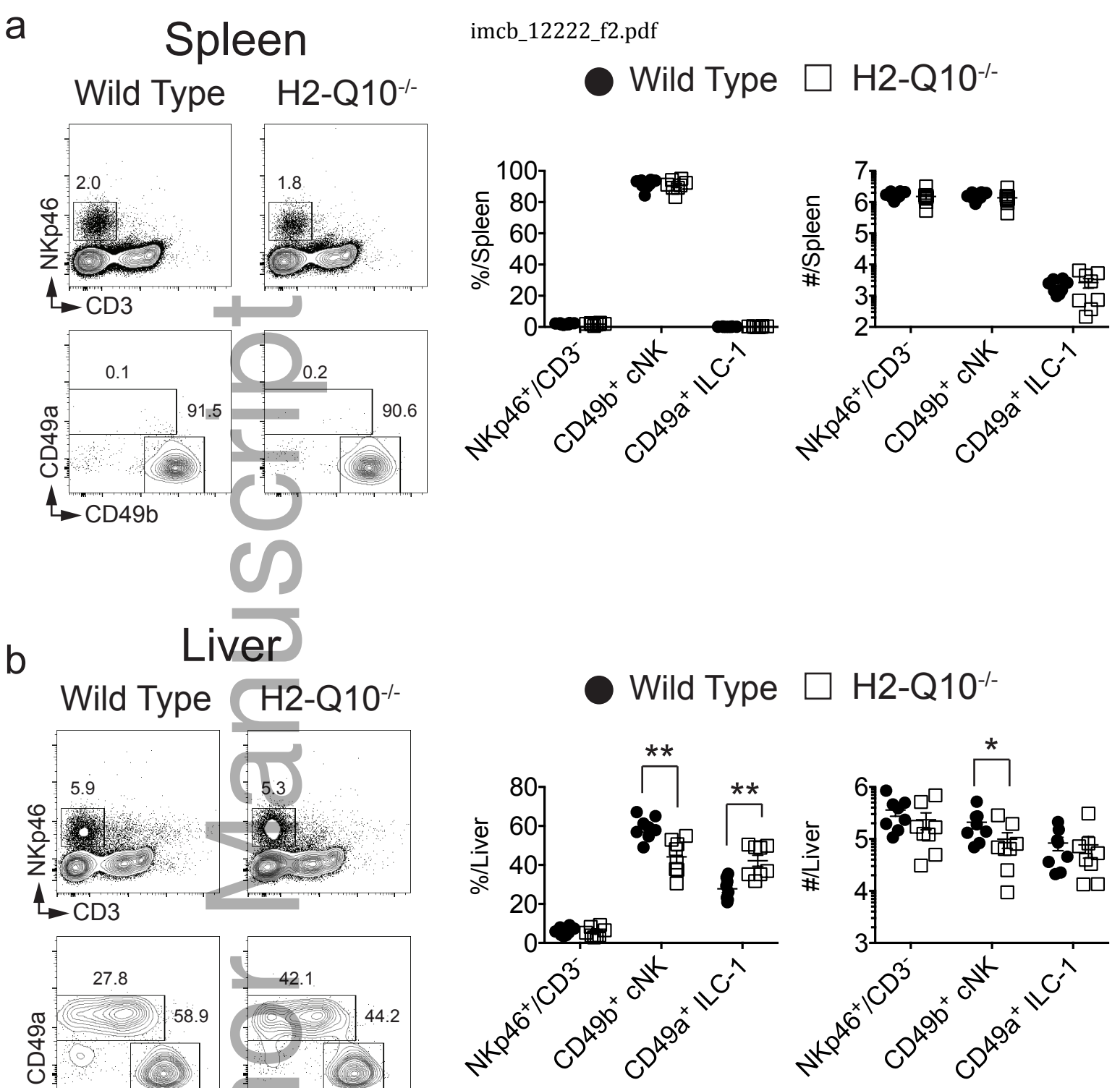

Figure 2 Goodall et al H2-Q10

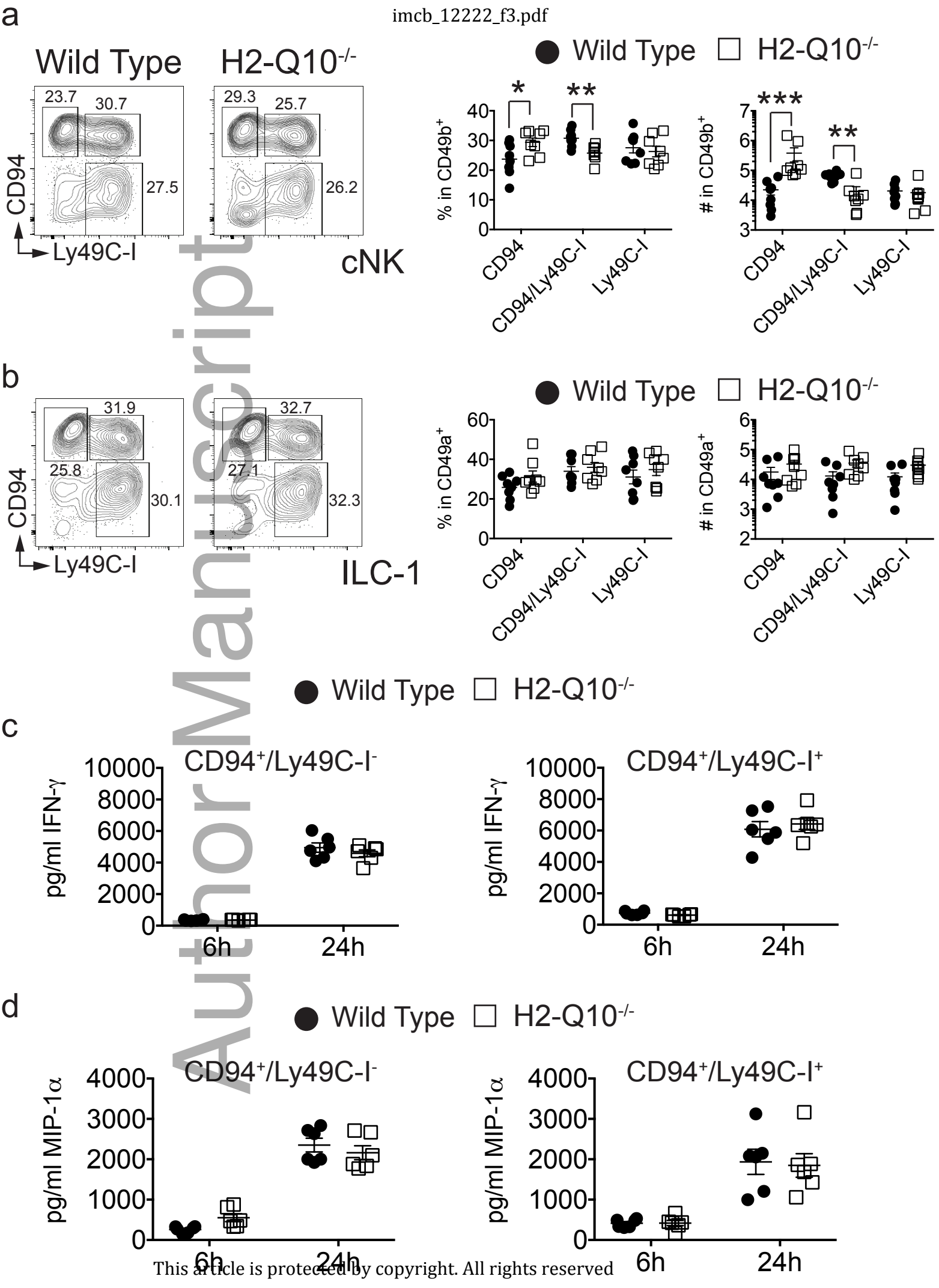

Figure 3 Goodall et al H2-Q10

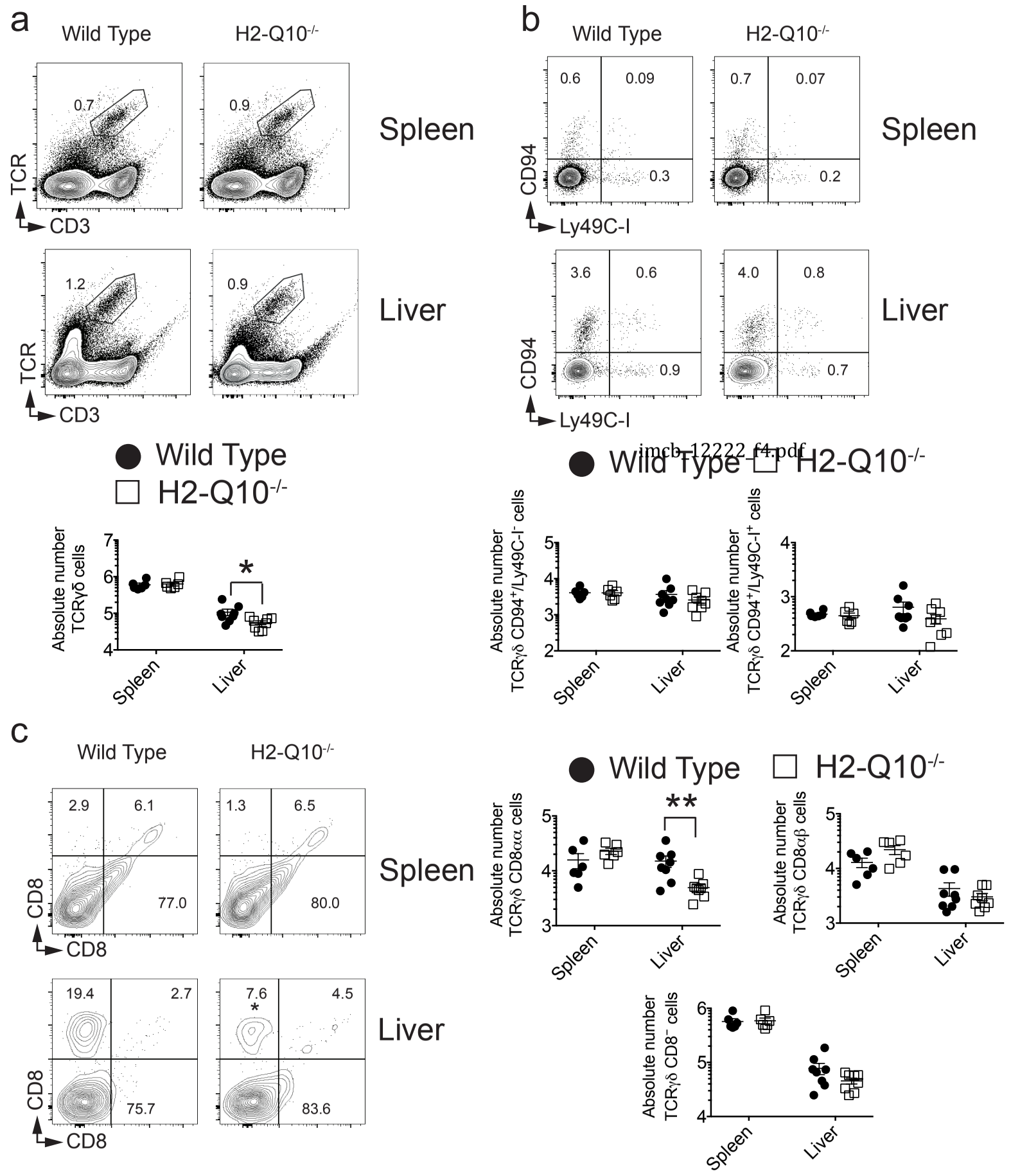

Figure 4 Goodall et al H2-Q10

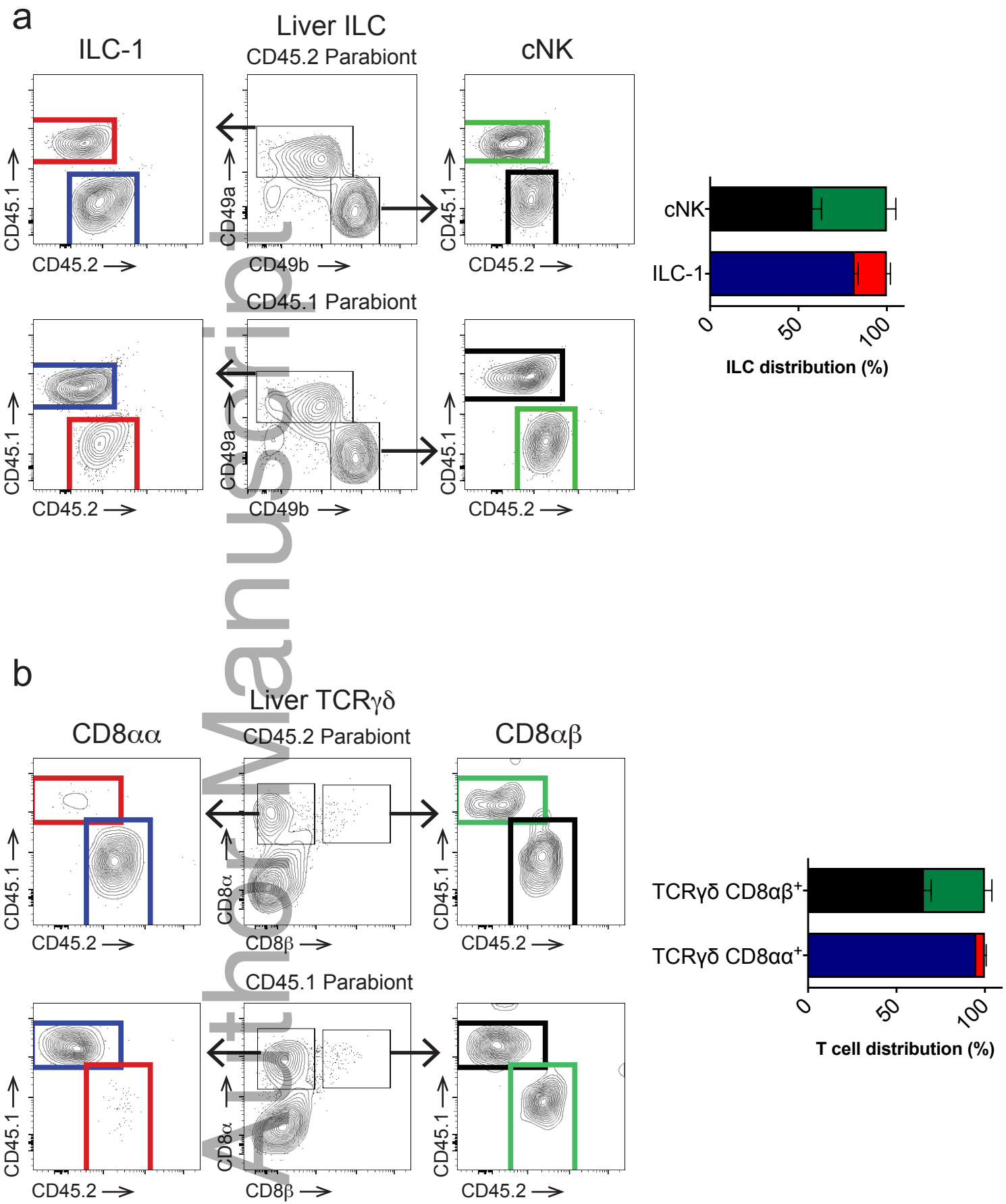

Figure 5 Goodall et al H2-Q10

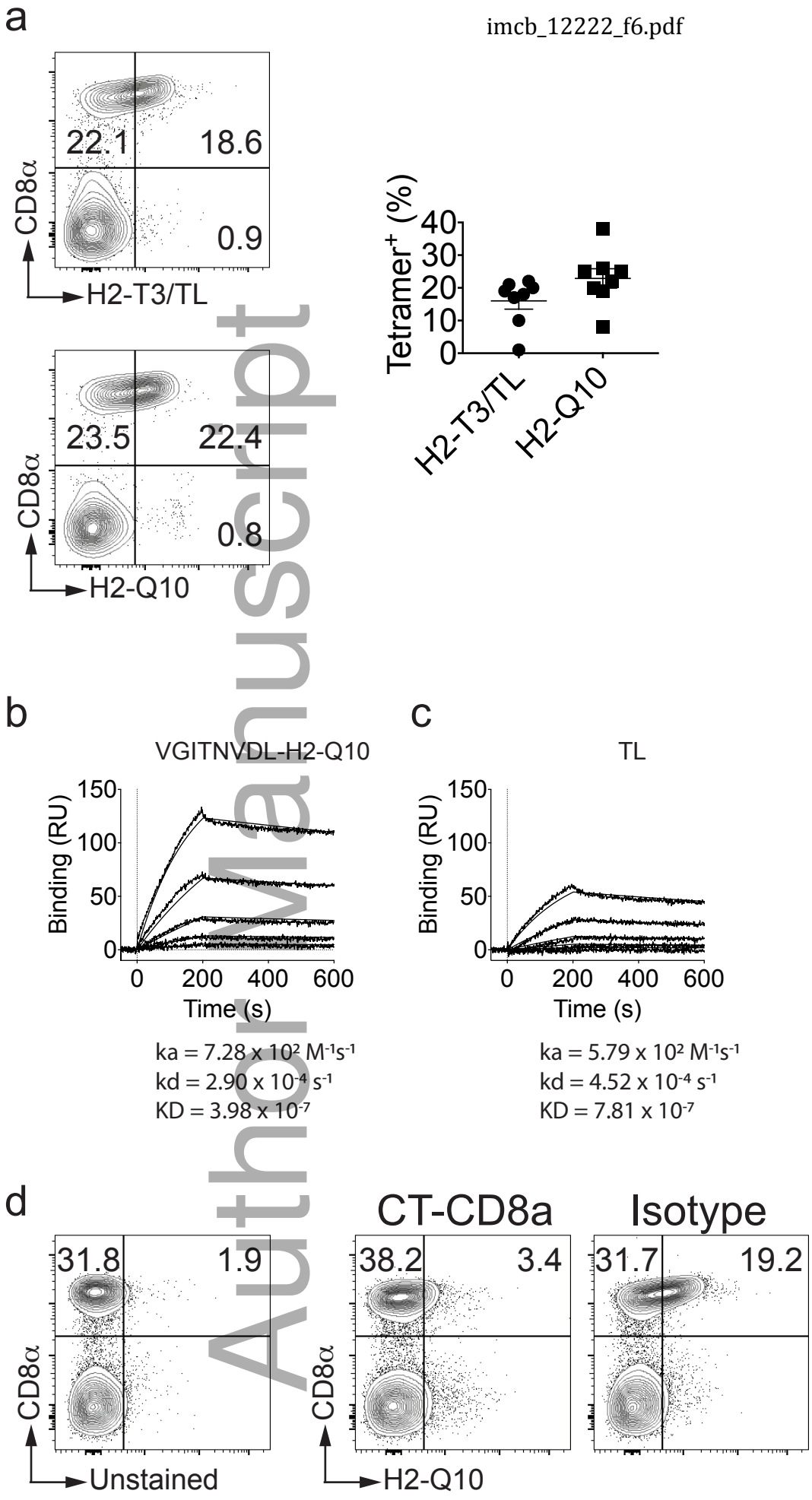

Figure 6 Goodall et al H2-Q10